INTERNATIONAL JOURNAL OF CLIMATOLOGY
Int. J. Climatol. **28**: 1879–1887 (2008)
Published online 29 February 2008 in Wiley InterScience
(www.interscience.wiley.com) DOI: 10.1002/joc.1689

Tree-ring based drought reconstruction in the central Hengduan Mountains region (China) since A.D. 1655

Ze-Xin Fan,[a,b] Achim Bräuning[b]* and Kun-Fang Cao[a]
[a] *Xishuangbanna Tropical Botanical Garden, the Chinese Academy of Sciences 88 Xuefu Road, Kunming 650223, China*
[b] *Institute of Geography, University of Erlangen-Nuremberg Kochstrasse 4/4, D-91054 Erlangen, Germany*

ABSTRACT: We developed four tree ring-width chronologies of three species (*Picea likiangensis* Pritz, *Tsuga dumosa* (D. Don) Eichler and *Abies ernestii* Rehd.) in the central Hengduan Mountains, north-western Yunnan, China. Although the four chronologies come from different species, significant correlations exist among the chronologies (mean $r = 0.47$), and the first principal component accounts for 60.5% of total variance over their common period 1655–2005. Correlation and response function analyses showed that pre-monsoon (March, April) precipitation and relative humidity and Palmer drought severity index (PDSI) have positive effects on radial growth, while temperature in March influences tree growth negatively. This indicates that tree growth is generally limited by spring-moisture availability. The spring (March–May) drought reconstruction was verified with independent data, and accounts for 42% of the actual PDSI variance during their common period 1951–2000. Wet springs occurred during AD 1690s, 1715–1730, 1750s, 1780s, 1825–1850, 1900s, 1930–1960, and 1990–present. Dry springs occurred during AD 1700–1715, 1733–1745, 1790–1820, 1860–1890, 1910–1925, and 1960–1990. Copyright © 2008 Royal Meteorological Society

KEY WORDS dendroclimatology; Hengduan Mountains; PDSI; tree rings

Received 5 June 2007; Revised 6 December 2007; Accepted 5 January 2008

1. Introduction

As a consequence of global warming, the summer temperature contrast between the Asian continent and the surrounding oceans is increasing. Consequently, global circulation models predict an increase in summer monsoon rainfall (Meehl and Washington, 1993; Hulme *et al.*, 1994; Böhner and Lehmkuhl, 2005). Comprehensive knowledge about the past monsoon behaviour can provide deeper insight into possible future circulation patterns. The Tibetan plateau has a mean elevation of more than 4000 m asl and covers an area of more than 2 million km^2. Thus, it acts as a heating surface during spring and summer and plays a key role in driving the Asian summer monsoon circulation (Murakami, 1987; Webster *et al.*, 1998). However, climate stations were not installed on the Tibetan plateau before 1950. This limits the analysis of long-term climate trends from meteorological records and requires the study of climate history from high-resolution proxy data like tree rings.

In recent years, considerable progress has been achieved in constructing century-to-millennial-long tree-ring chronologies from north-eastern Tibet (e. g. Zhang *et al.*, 2003; Sheppard *et al.*, 2004; Shao *et al.*, 2005; Gou *et al.*, 2006) and from the southern parts of the Tibetan Plateau (Wu and Zhan, 1991; Bräuning, 1994, 2001; Bräuning and Grießinger, 2006). Summer temperature and summer monsoon history in south-east Tibet were reconstructed from maximum latewood density (MLD) and stable carbon isotopes in several coniferous species (Helle *et al.*, 2002; Bräuning and Mantwill, 2004). However, only few studies have been conducted in the Hengduan Mountains (Wu *et al.*, 1988; Bräuning, 2001), which form the southern rim of the Tibetan plateau and are, therefore, strongly exposed to the South Asian summer monsoon. Based on tree ring-width data from the upper tree line and lower-altitude arid area, Wu *et al.* (1988) reported a reconstruction of fluctuations of air temperature and annual precipitation during the last 400 years, but no information about the strength of the tree growth-climate signal or the reliability of the reconstruction was provided. In addition, their study was based on a very short set of climate data and does not document environmental changes that occurred during the last two decades, a period of special interest.

Climate data from Deqin meteorological station (Figure 1) indicate that summer and winter temperatures have increased since the 1970s. Contemporaneously, a decreasing trend in summer precipitation is registered. In combination, these opposing trends seem to be a major cause for the observed retreat of glaciers in the area and for a rise of the upper tree line evidenced from repeat photographs (Baker and Moseley, 2007). Here, we present four new tree ring-width chronologies from the central Hengduan Mountains at the southern rim of the Tibetan

* Correspondence to: Achim Bräuning, Institute of Geography, University of Erlangen-Nuremberg Kochstrasse 4/4, D-91054 Erlangen, Germany. E-mail: abraeuning@geographie.uni-erlangen.de

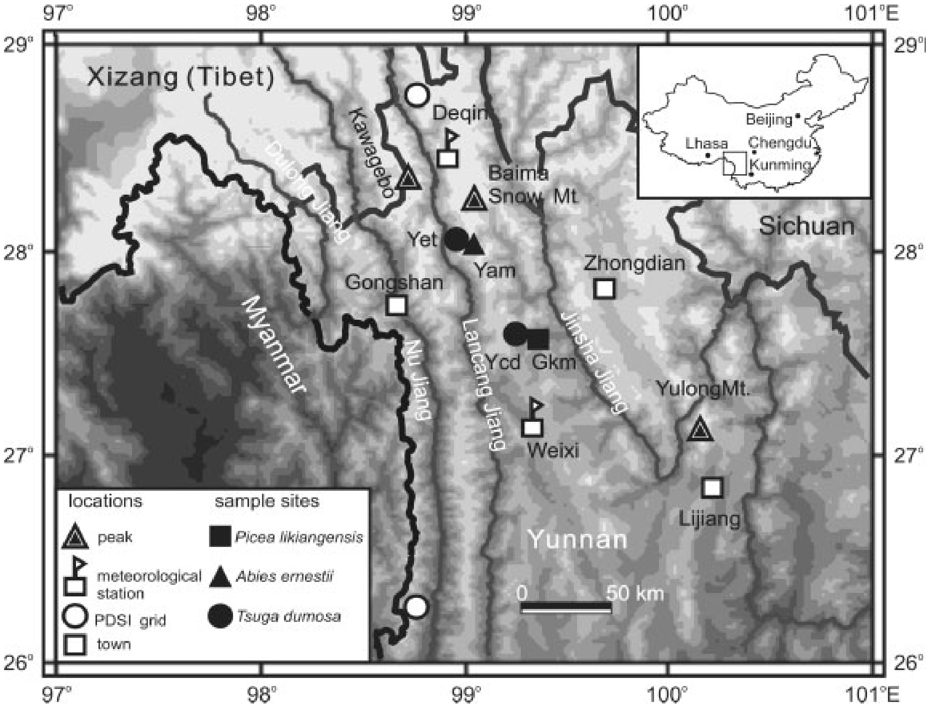

Figure 1. Map of the sampling sites in the central Hengduan Mountains, north-western Yunnan.

plateau. We analyse the relationships between the tree growth and climatic variables to examine the regional climate variability during the past 350 years.

2. Study area

The Baima Snow Mountain is located in the central Hengduan Mountain range in north-western Yunnan Province, China (Figure 1). Biogeographically, the area is in a transitional zone between the south-eastern Tibetan Plateau and the north-western edge of the Yunnan Plateau. The Hengduan Mountains were not completely covered by ice in the Pleistocene, making them a refuge area for plant species and wildlife. Thus, the region is one of the hot spots of plant biodiversity in the world (Frenzel *et al*., 2003). Four of Asia's major rivers, the Jinsha Jiang (upper Yangtse), Lancang Jiang (upper Mekong), Nu Jiang (upper Salween), and Dulong Jiang (tributary of the Irrawaddy) converge within a 90 km corridor in this portion of Hengduan Mountain range. The resulting landscape patterns include extreme topographic gradients between deeply incised parallel gorges in *ca* 1500 m elevation and glaciated peaks (>6700 m asl) within a distance of 20 km or even less. As a consequence, distinct altitudinal belts of different vegetation types occur. These gorges form passage ways for the monsoonal air masses to penetrate into the dry interior of Tibet (Chang, 1981).

3. Materials and methods

3.1. Chronology development

The four chronologies presented in this study come from three coniferous tree species, i.e. *Picea likiangensis* Pritz, *Tsuga dumosa* (D. Don) Eichler, and *Abies ernestii* Rehd. Increment cores from 98 trees (148 cores) were extracted with an increment borer at four sites on the west-facing slopes of the Baima Snow Mountains, NW Yunnan (Figure 1). The forests at the sampling sites are hardly disturbed by human activity. They have old-growth characteristics including many large and old trees and many snags, and a dense crown cover of 50–60%. At each site, a minimum of 16 trees were cored at breast height.

After air-drying, the surface of the cores was prepared with razor blades and the surface contrast was enhanced with chalk. Ring widths were registered with a LINTAB measuring system with a resolution of 0.01 mm, and all cores were cross-dated by visual growth pattern matching, skeleton plotting and statistical tests (sign-test and t-test) in the software package TSAP (Stokes and Smiley, 1968; Rinn, 1996). Some cores of poor quality (e.g. fragmented, rotten, and not cross-datable) were discarded from further analyses. Finally, 136 increment cores from 93 trees were selected, while 12 cores were excluded.

The final chronologies were developed with the ARSTAN program (Cook, 1985). The raw ring-width series were standardized to remove biological growth trends while preserving growth variations that are probably related to climate variability. Prior to standardization, the variance of each series was stabilized using a data-adaptive power transformation based on the local mean and standard deviation (Cook and Peters, 1997). Standardization was carried out in two steps. After fitting a negative exponential or a linear regression curve of the negative slope, the tree-ring sequences were detrended with a cubic smoothing spline with a

DOI: 10.1002/joc

50% frequency-response cutoff equal to 67% of the series length. The final tree-ring index chronologies were obtained by calculating differences between the transformed ring-width measurements and the fitted splines. All detrended series were averaged to chronologies by computing the biweight robust mean in order to reduce the influence of outliers (Cook and Kairiukstis, 1990). To reduce the potential influence of decreasing sample depth with increasing age, the variance of the chronology was stabilized (Osborn *et al.*, 1997). We produced two versions of each chronology. The first version is a standard chronology where low-order persistence has been retained, the second version is the pre-whitened or residual chronology where significant low-order persistence has been removed (Cook, 1985).

Signal strength of the site chronologies was assessed by the mean inter-series correlation (Rbar) and the expressed population signal (EPS, Wigley *et al.*, 1984). EPS is a function of Rbar and the sample size and estimates the variance fraction of an infinite, hypothetical population expressed by the chronology. A level of 0.85 in EPS is considered to indicate a satisfactory quality of a chronology. Both Rbar and EPS were calculated for 30-year moving windows with 15-year overlaps along the chronology.

3.2. Climate data

There are two meteorological observation stations, relatively close to the sampling sites (Figure 1), located in Deqin (28.48 °N, 98.92 °E, 3320 m asl, record length 1957–2000), and Weixi (27.17 °N, 99.28 °E, 2325 m asl, record length 1961–2000). The region's climate is temperate and is characterized by a rainfall maximum during the summer months (Figure 2). Summer rains originate from monsoonal air masses flowing over the Bay of Bengal; whereas winters are generally dry (Xu *et al.*, 2003). A second rainfall maximum, which is more pronounced at Weixi than at Deqin, occurs during spring (February–April). The mean annual temperature at Deqin is 5.2 °C, with a mean temperature of 12.3 °C in July and −2.5 °C in January. Mean annual total precipitation is 644 mm. The mean annual temperature at Weixi is 11.5 °C and annual rainfall is 962 mm (Figure 2). Deqin is located north of the highest peaks of Baima Snow Mountain and Kawagebo (Figure 1); the rain shadow effect results in less precipitation at Deqin than at Weixi, despite the higher elevation of the former. The Palmer drought severity index (PDSI; Palmer, 1965) measure the moisture conditions by incorporating precipitation, soil moisture demand and supply into a primitive hydrological accounting system. A dataset for the PDSI on a 2.5° × 2.5° grid was developed by Dai *et al.* (2004). The two grid points next to our sampling sites (26.25 °N, 98.75 °E and 28.75 °N, 98.75 °E) were used for detecting the growth response to moisture conditions. A regional series of climate data was created from the two meteorological stations for their common period of 1961–2000, and from the two PDSI grid points for 1951–2000, by applying the methods described by Jones and Hulme (1996).

3.3. Growth–climate response

An inter-site comparison of the four tree-ring index chronologies was assessed by creating a correlation matrix over the common period 1655–2005. In addition, a principal component analysis (PCA) was carried out, which involves the extraction of orthogonal (uncorrelated) principal components from an original set of correlated variables by employing a variance maximizing rotation of the original variable space (Richman, 1986). The first principal component (PC1) represents the common variance of the chronology set and thus indicates the regional growth signal.

The climate–growth relationships were examined by computing correlations (Blasing *et al.*, 1984) between station climate data and tree-ring index chronologies. Pearson correlations coefficients were calculated between the ring-width chronologies and the monthly series of temperature and precipitation from both Weixi (1961–2000) and Deqin station (1957–2000), for a 15-month period ranging from July of the summer prior to growth until September of the growth year. The bootstrapped correlation and response functions were performed to analyse the relationships between PC1 and regional

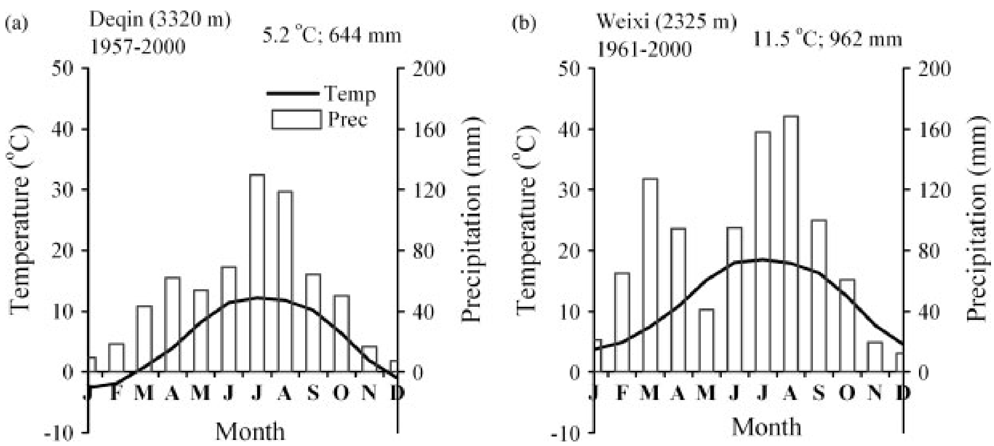

Figure 2. Climate diagrams for the meteorological stations of Deqin and Weixi in north-western Yunnan.

DOI: 10.1002/joc

climatic variables (Biondi and Waikul, 2004). PC1 was compared with the regional climate series (precipitation, temperature, relative humidity and PDSI) for a 15-month period from July of the summer prior growth to September of the growth year.

4. Results

Descriptive statistics of the four standard chronologies are shown in Table I. All chronologies exceed 460 years and one 613-year-old tree (*Tsuga dumosa*) was found at Yet site. The average mean sensitivity (a measure of the inter-annual variability in tree-ring series) at all sites was around 0.18, indicating that the ring-width chronologies show relative low inter-annual variability, which is characteristic for trees growing in humid environments. First-order autocorrelation ranged from 0.66 to 0.71, which documents that the chronologies contain low-frequency variance generated by climate and by tree-physiological lag effects. The latter include needle retention and the remobilization of stored food reserves for growth in the following spring (Fritts, 1976). The Rbar and EPS statistics of the site chronologies signal strength ranged from 0.28 to 0.37 and from 0.77 to 0.87, respectively. Three site chronologies meet the 0.85-EPS criterion after AD 1655, except for site Yet whose EPS was above 0.75 at 1655 and reached the 0.85 limit only after 1685 (Figure 3(d)). Nevertheless, we regarded the period 1655–2005 (351 years) as common period of acceptable chronology quality for further analyses.

Despite of the different species analysed, the four chronologies correlated to each other significantly over the common period 1655–2005, with correlation coefficients ranging from 0.40 to 0.55 ($p < 0.01$) (Table II). Ring-width patterns were very similar among the four chronologies, especially concerning high and middle frequency growth variations (Figure 3). The average cross-chronology correlation (calculated for a 30-year moving window)was 0.47 ($p < 0.001$) over 1655–2005, and ranged from 0.20 to 0.66 (Figure 7(a)).

The PCA of the four residual chronologies showed that only the eigenvalue of PC1 was greater than one and that PC1 accounts for 60.5% of the total variance. The four chronologies showed common positive loadings on PC1: 0.78 for Gkm, 0.79 for Ycd, 0.75 for Yam and 0.79 for Yet, respectively. Therefore, PC1 reflects the common growth response to regional climatic variations, and the score of PC1 can be used to evaluate the regional climate-growth relationships and to indicate regional climate variability. Other PCs were insignificant, and can probably be assigned to small-scale growth variations caused by site-specific growth reactions or local growth disturbances.

Table II. Correlation matrix of the four ring-width chronologies for the common period 1655–2005.

	Gkm	Ycd	Yam	Yet
Gkm	1.00	0.55	0.44	0.44
Ycd		1.00	0.40	0.49
Yam			1.00	0.52
Yet				1.00

The site codes are identical with those in Table I. All correlations are significant at $p < 0.01$.

Correlation analyses indicated that tree growth was mainly affected by early spring precipitation, especially during January, March and May (Figure 4). The correlation coefficients between regional seasonal precipitation (March–May) and the residual ring-width index chronologies were significant ($p < 0.05$) except for site Yet ($r = 0.53$ for Gkm, 0.47 for Ycd, 0.37 for Yam, and 0.29 for Yet). Compared with the other two species, the radial growth of *Tsuga dumosa* showed a weaker (positive) spring-precipitation response, but stronger (negative) response to temperatures (Figure 4(c), (d)). When standard chronologies instead of residual chronologies are compared with climate parameters, we found the same general patterns but lower correlations (not shown). The correlation coefficients were mostly positive between the PC1 of the four residual chronologies and regional monthly precipitation, relative humidity and PDSI (Figure 5(a), (c), (d)), but negative between PC1 and regional monthly temperature (Figure 5(b)). Response-function analyses indicated that the water availability in March and April was a crucial factor

Table I. Site locations and chronology statistics.

Site	Lat./Lon. (degree)	Elev (m)	Trees (cores)	Period	MSL (year)	AGR[a] (mm)	MS[b]	AC1[b]	Rbar[c]	EPS[c]
Gkm	27.58/99.35	3240	28 (38)	1429–2005	285	1.30	0.19	0.69	0.31	0.85
Ycd	27.59/99.29	3150	32 (49)	1542–2005	222	1.34	0.19	0.71	0.28	0.85
Yam	28.04/99.02	3200	17 (19)	1489–2005	273	1.09	0.18	0.66	0.37	0.87
Yet	28.04/98.98	3100	16 (30)	1393–2005	297	1.08	0.17	0.69	0.28	0.77

Gkm: *Picea likiangensis*; Yam: *Abies ernestii*; Ycd and Yet: *Tsuga dumosa.*

Lat, latitude; Lon, longitude; Elev, Elevation; MSL, mean segment length (tree age); AGR, average growth rate; MS, mean sensitivity; AC1, first-order autocorrelation; Rbar, mean inter-series correlation; EPS, expressed population signal.

[a] Calculated for raw ring-width values.

[b] Calculated for ARSTAN standard chronologies.

[c] Calculated for ARSTAN standard chronologies for 30-years intervals with 15-year overlaps.

DOI: 10.1002/joc

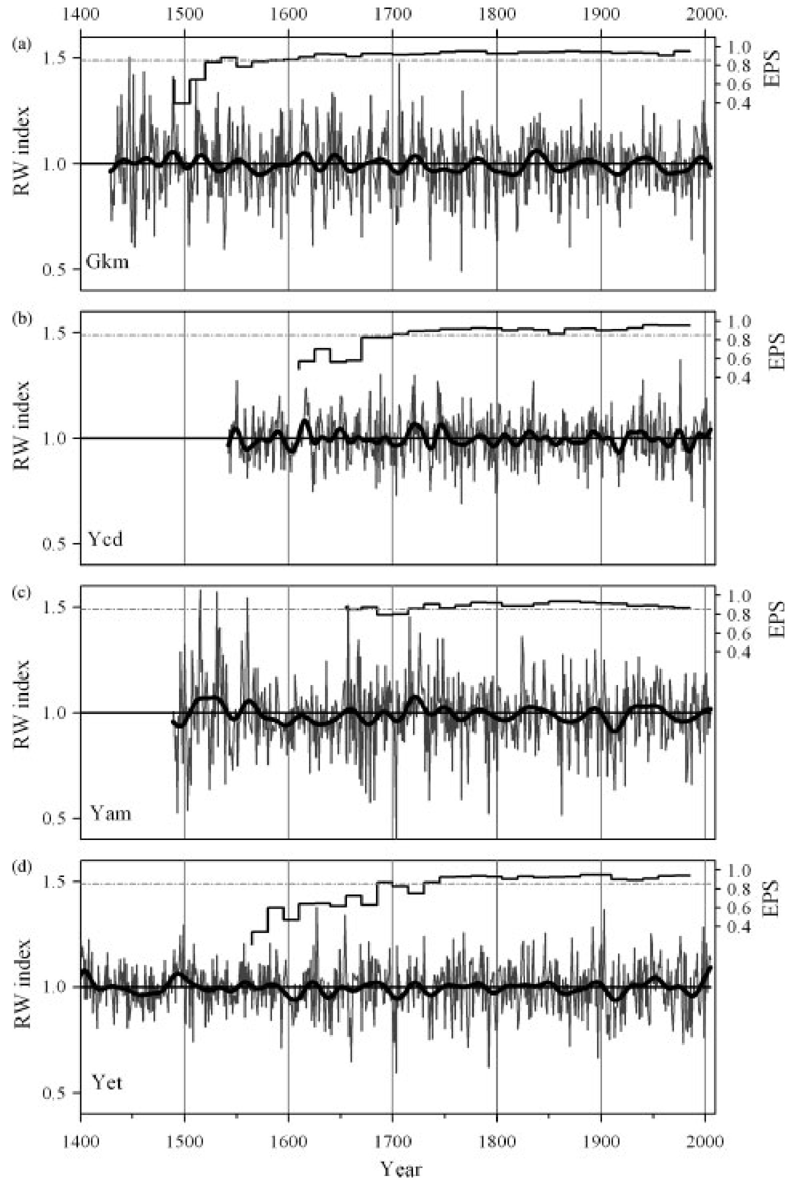

Figure 3. The four residual chronologies from Baima snow mountains, NW Yunnan. The expressed population signal (EPS) statistic through time is shown in the upper section of each graph. Thin lines represent annual values; bold lines were smoothed with an 11-year-FFT filter (fast Fourier transform) to emphasize long-term growth variations. The site codes match with those of Table I.

impacting radial growth. The highest correlation between PC1 and PDSI occurred for the season March–May ($r = 0.65$, $p < 0.01$) which was therefore reconstructed by using PC1 of the four residual chronologies as predictor variable.

A linear regression model ($Y = 0.818X - 0.0724$) was developed to reconstruct the drought history for the central Hengduan Mountain region. During the common period of tree rings and PDSI data (1951–2000), the reconstruction accounted for 42% of the actual PDSI variance (Table III). The spring PDSI estimates derived from this model agreed well with the yearly departures from the long-term mean in the observed data (Figure 6). Split-sample calibration-verification and leave-one-out cross-verification methods (Michaelsen, 1987) were employed to evaluate the statistical fidelity of this model. The reduction error (RE) and the coefficient of efficiency (CE) were positive; indicating significant skill in the tree-ring estimates (Fritts, 1976). The results of the sign-test and product mean test demonstrated the validity of our regression model (Table III).

The spring (March–May) PDSI reconstruction (Figure 7(b)) showed that wet periods prevailed in the 1690s, 1715–1730, 1750s, 1780s, 1825–1850,1900s, 1930–1960, and 1990–present. Extremely wet years ($\geq$2SD) occurred in AD 1703, 1824, 1835, 1940, and 1998. In contrast, the intervals AD 1700–1715, 1733–1745, 1790–1820, 1860–1890, 1910–1925, and 1960–1990 were relatively dry. Extremely dry years ($\leq$2SD) were more frequent than extremely wet years and were concentrated during AD 1730–1800 and 1870–1900, and after 1980. From the higher mean correlation between the four individual chronologies (Figure 7(a)), it can be concluded that these were time

DOI: 10.1002/joc

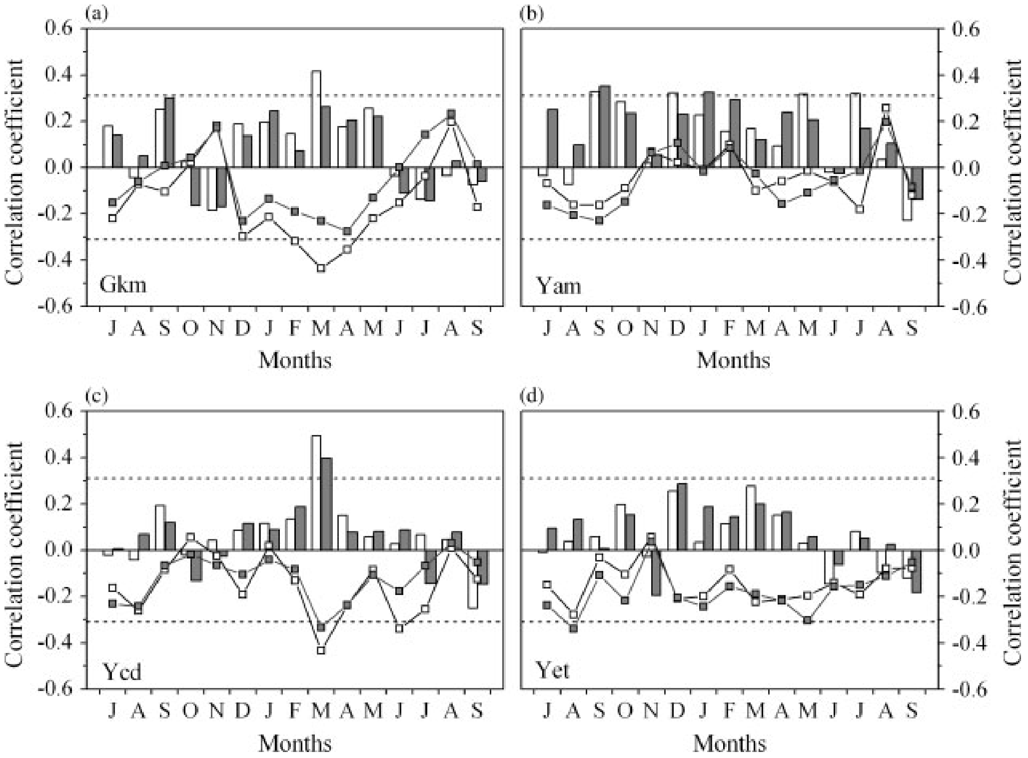

Figure 4. Correlation coefficients between radial growth and monthly mean temperature (dot-lines) and total monthly precipitation (columns) at nearby meteorological stations of Deqin (gray) and Weixi (white). Correlations are computed from the previous year July to the current year September over 1957–2000 for Deqin and 1961–2000 for Weixi. Horizontal dashed lines denote the 95% levels of significance.

Table III. Statistics of calibration-verification test results for the common period 1951–2000.

Split-sample calibration-verification								
Calibration				Verification				
Period	*R*	R^2	*F*	Period	Sign-test	Pmt	RE	CE
1951–1980	0.65	0.42	20.4**	1981–2000	14/6**	2.50**	0.318	0.298
1981–2000	0.68	0.47	15.9**	1951–1980	22/8*	2.51**	0.374	0.359
1951–2000	0.65	0.42	34.5**					
Leave-one-out verification								
1951–2000	0.61				38/12**	2.75**	0.372	

* Significant at $p < 0.05$,
** Significant at $p < 0.01$
R is correlation coefficient; Sign-test is sign of paired observed and estimated departures from their mean on the basis of the number of agreements/disagreements; Pmt is product mean test; RE is the reduction of error, any positive value indicates that there is some sense in the reconstruction (Fritts, 1976); CE is the coefficient of efficiency.

periods of strong climatic forcing of regional tree-growth patterns. Particularly, dry years occurred in AD 1670, 1706, 1735–1736, 1757, 1766, 1772, 1792, 1800, 1820, 1870, 1887, 1897, 1987, and 1999.

5. Discussion

We found significant positive correlations between tree growth and precipitation in January, March and May (Figure 4). The correlation and response functions results between PC1 and climate variables also indicated that the spring-moisture availability was a major limiting factor for tree-ring growth (Figure 5). It is interesting to note that the seasonal rainfall distribution (Figure 2) shows a secondary rainfall maximum during March–May, just before the onset of summer monsoon season (June–September). This rainfall probably originates from local circulation patterns and accounts for 27 and 25% of total annual precipitation at Weixi and at Deqin, respectively. In southern Tibet, dry and warm conditions before the onset of the summer monsoon cause drought stress to the trees and are thus limiting growth (Bräuning, 1999; Bräuning and Grießinger, 2006). Thus,

DOI: 10.1002/joc

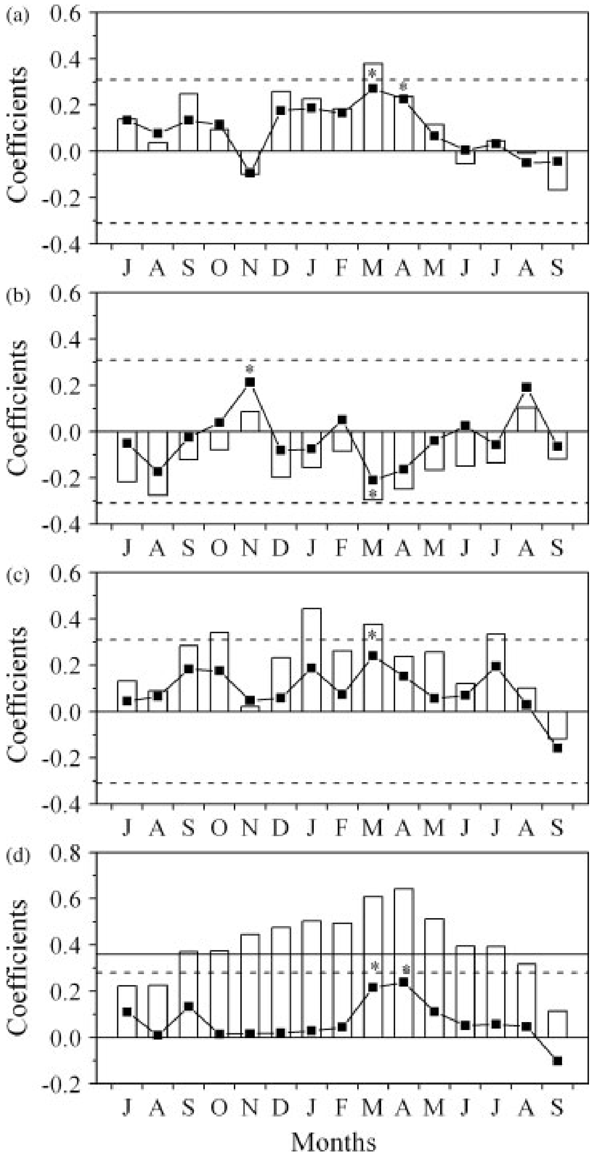

Figure 5. Correlation (columns) and response function (dot-lines) coefficients between the first principal component (PC1) of the residual chronologies and regional monthly (a) total precipitation, (b) mean temperature, (c) relative humidity for 1961–2000, and (d) PDSI data for 1951–2000. The coefficients were calculated from the previous year July to the current year September. Horizontal dashed and bold lines denote 95 and 99% significance levels, respectively. The asterisks indicate the 95% significance level for response functions based on bootstrap tests.

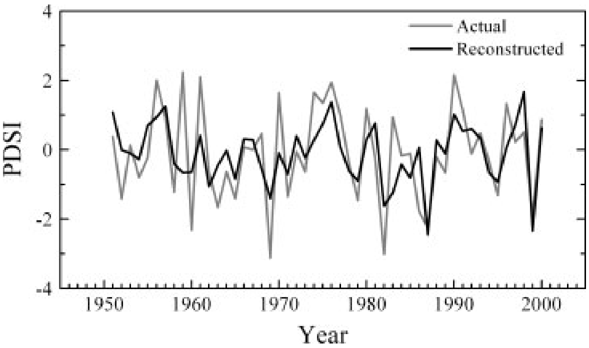

Figure 6. Actual (gray) and reconstructed (dark) March–May PDSI during their common period 1951–2000. The estimation explains 42% of the actual PDSI variance in this common period.

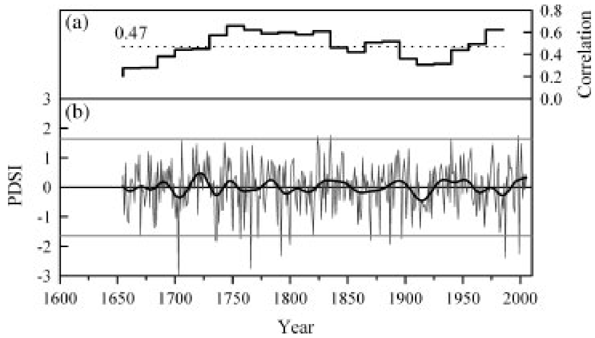

Figure 7. (a) Average cross-chronology correlation (mean is 0.47) of the four residual chronologies, calculated for 30-year periods with 15-year overlaps. (b) The reconstruction of March–May PDSI in the central Hengduan Mountain region over the past 350 years. The thin line represents the annual value and the thick line was smoothed with a 11-year FFT-filter (Fast Fourier Transform) to emphasize long-term fluctuations. The gray line indicates the ±2SD values.

tree-growth benefits from the former winter and current spring precipitation, which increase the soil moisture content during the early part of the growing season. Later on, after the onset of the summer monsoon season, enough moisture is available to satisfy the water demand of the trees.

Most of the correlations between tree growth and temperature were negative, especially at the two *Tsuga dumosa* sites. High temperatures during the growing season enhance evapotranspiration and thus decrease soil moisture availability (LeBlanc and Terrell, 2001). This growth response is not surprising for trees growing on steep slopes in a subtropical climate. Our study sites are located at middle elevations, far away from the upper tree line which lays around 4200 m asl in the Baima Mountain region.

Although our PDSI reconstruction was based on the residual tree-ring chronologies, considerable decadal scale moisture variability was retained in our reconstruction. The dry springs in the 1700s, 1730s and 1790s–1820s (Figure 7(b)) were also detected as dry periods in the same area by Wu *et al*. (1988). The dry periods in the 1800s are synchronous with dry conditions in Mongolia and in the western Himalaya (Pederson *et al*., 2001; Singh *et al*., 2006). Other intervals in the 18th century were relative wet, especially the period 1715–1730. The period 1825–1850 was a relatively prolonged wet period, and abrupt growth increases occurred in 1824–1825, 1835–1836, and in 1846. This period has also been reported as a prolonged phase with wet springs (AD. 1820s–1840s) in the western Himalayan region of India (Singh *et al*., 2006). The most severe drought period in the past 350 years occurred during 1910–1925. This severe drought has also been recorded in tree-rings from North China (Li *et al*., 2006; Liang *et al*., 2006) and southern Tibet (Bräuning and Grießinger, 2006). Liang *et al*. (2006) combined tree-ring records and historical records (meteorological, hydrological and documentary

DOI: 10.1002/joc

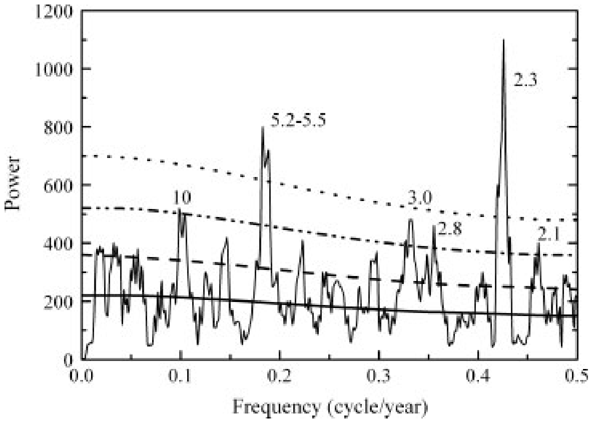

Figure 8. Multi-Taper method (MTM) power spectra of the reconstructed spring Palmer drought severity index (PDSI). The bold line indicates the null hypothesis; the dash, dash-dot, and dotted lines indicate the 90, 95 and 99% significance level, respectively.

evidence) and reported that the 1920s drought was severe and sustained. It extended across north China, southern Ningxia, eastern Qinghai, Gansu and eastern Xinjiang in north-west China. Spring climate was relatively wet from 1930 to 1960, which was also reported by Wu *et al.* (1988). The period 1960–1990 was relatively dry, especially 1983–1988, which coincides with reports about a regional drought disaster in 1986 by the county annals of Deqin (The Editing Committee of 'The annals of Deqin County', 1997). The last *ca* 15 years were comparatively wet, but were still within the range of fluctuations over the last 350 years. Multi-taper method (MTM) spectral analysis (Mann and Lees, 1996) was used to evaluate frequency domains in local drought variability (Figure 8). A decadal broadband power was identified at 10 years ($p < 0.05$), which resembles other findings from Mongolia and northern China and suggests an influence of solar forcing (Pederson *et al.*, 2001; Li *et al.*, 2006). Significant high-frequency peaks were found at 2.3 years and 5.2–5.5 years ($p < 0.01$), as well as at 2.1, 2.8, and 3.0 years ($p < 0.05$). These periods fall within the range of variability of the El Nino–Southern Oscillation (ENSO). The latter has been found to have strong, but variable influence on the strength of the South Asian summer monsoon system (e.g. Charles *et al.*, 1997; Kane, 2006). Thus, like in other annually resolved climate archives from the Tibetan plateau (e.g. in ice cores) (Yang *et al.*, 2000), ENSO variability might be reflected in the long-term growth curves of moisture-sensitive trees. However, this point needs further investigation concerning sample density and climate-growth analyses.

Acknowledgements

The authors thank Mrs. Iris Burchardt for her aid on ring-width measurements. Climate data were provided by the National Meteorological Information Centre (NMIC). The work was financially supported by the National Natural Science Foundation of China (No. 90302013) and the Max–Planck–Gesellschaft.

References

Baker BB, Moseley RK. 2007. Advancing treeline and retreating glaciers: implications for conservation in Yunnan, P.R. China. *Arctic Antarctic and Alpine Research* **39**(2): 200–209.

Biondi F, Waikul K. 2004. DENDROCLIM2002: A C++ program for statistical calibration of climate signals in tree-ring chronologies. *Computers & Geosciences* **30**(3): 303–311.

Blasing TJ, Solomon AM, Duvick DN. 1984. Response functions revisited. *Tree-Ring Bulletin* **44**: 1–15.

Böhner J, Lehmkuhl F. 2005. Environmental change modelling for Central and High Asia: pleistocene, present and future scenarios. *Boreas* **34**: 220–231.

Bräuning A. 1994. Dendrochronology for the last 1400 years in Eastern Tibet. *GeoJournal* **34**(1): 75–95.

Bräuning A. 1999. Dendroclimatological potential of drought-sensitive tree stands in Southern Tibet for the reconstruction of the monsoonal activity. *IAWA Journal* **20**(3): 325–338.

Bräuning A. 2001. Climate history of the Tibetan Plateau during the last 1000 years derived from a network of Juniper chronologies. *Dendrochronologia* **19**(1): 127–137.

Bräuning A, Mantwill B. 2004. Summer temperature and summer monsoon history on the Tibetan plateau during the last 400 years recorded by tree rings. *Geophysical Research Letters* **31**: L24205, Doi: 10.1029/2004GL020793.

Bräuning A, Grießinger J. 2006. Late Holocene variations in monsoon intensity in the Tibetan–Himalayan region-evidence from tree rings. *Journal of the Geological Society of India* **69**(3): 485–494.

Chang DHS. 1981. The vegetation zonation of the Tibetan Plateau. *Mountain Research and Development* **1**(1): 29–48.

Charles CD, Hunter DE, Fairbanks RG. 1997. Interaction between the ENSO and the Asian monsoon in a coral record of tropical climate. *Science* **277**: 925–928.

Cook ER. 1985. A time-series analysis approach to tree-ring standardization, PhD dissertation, The University of Arizona Press, Tucson.

Cook ER, Kairiukstis LA. 1990. *Methods of Dendrochronology*. Kluwer Academic Press: Netherlands.

Cook ER, Peters K. 1997. Calculating unbiased tree-ring indices for the study of climatic and environmental change. *The Holocene* **7**: 361–370.

Dai AG, Trenberth KE, Qian T. 2004. A global dataset of Palmer Drought Severity Index for 1870–2002: relationship with soil moisture and effects of surface warming. *Journal of Hydrometeorology* **5**: 1117–1130.

Frenzel B, Bräuning A, Adamczyk S. 2003. On the problem of possible last-glacial forest-refuge-areas within the deep valleys of Eastern Tibet. *Erdkunde* **57**: 182–198.

Fritts HC. 1976. *Tree Rings and Climate*. Academic Press: London.

Gou XH, Chen FH, Yang MX, Jacoby G, Peng JF, Zhang YX. 2006. A comparison of tree-ring records and glacier variations over the past 700 years, northeastern Tibetan Plateau. *Annals of Glaciology* **43**: 86–90.

Helle G, Schleser GH, Bräuning A. 2002. Climate history of the Tibetan Plateau for the last 1500 years as inferred from stable isotopes in tree rings. In *Proceeding of the International Conference on the Study of Environmental Change Using Isotope Techniques, IAEA CN–80–80*, Vienna 22–27–04–2001, 301–311.

Hulme M, Zhao Z, Jiang T. 1994. Recent and future climatic change in East Asia. *International Journal of Climatology* **14**: 637–658.

Jones PD, Hulme M. 1996. Calculating regional climatic time series for temperature and precipitation: methods and illustrations. *International Journal of Climatology* **16**: 361–377.

Kane RP. 2006. Unstable ENSO relationship with Indian regional rainfall. *International Journal of Climatology* **26**: 771–783.

LeBlanc D, Terrell M. 2001. Dendroclimatic analyses using Thornthwaite–Mather–Type evapotranspiration models: a bridge between dendroecology and forest simulation models. *Tree-Ring Research* **57**(1): 55–66.

Li JB, Cheng FH, Cook ER, Guo XH, Zhang YX. 2006. Drought reconstruction for north central China from tree rings: the value of the Palmer drought severity index. *International Journal of Climatology* **27**: 903–909.

Liang EY, Liu XH, Yuan YJ, Qin NS, Fang XQ, Huang L, Zhu HF, Wang LL, Shao XM. 2006. The 1920s drought recorded by tree rings and historical documents in the semi-arid and arid area of Northern China. *Climatic Change* **79**: 403–432.

Mann ME, Lees J. 1996. Robust estimation of background noise and signal detection in climatic time series. *Climatic Change* **33**: 409–445.

Meehl GA, Washington WM. 1993. South Asian summer monsoon variability in a model with doubled atmospheric carbon dioxide concentration. *Science* **260**: 1101–1104.

Michaelsen J. 1987. Cross–validation in statistical climate forecast models. *Journal of Climate and Applied Meteorology* **26**: 1589–1600.

Murakami T. 1987. Effects of the Tibetan Plateau. In *Monsoon Meteorology*, Vol. 7, Chang C-P, Krishnamurti TN (eds). Oxford University Press: New York; 235–270.

Osborn TJ, Briffa KR, Jones PD. 1997. Adjusting variance for sample size in tree-ring chronologies and other regional mean timeseries. *Dendrochronologia* **15**: 89–99.

Palmer WC. 1965. *Meteorological Drought. Weather Bureau Res. Paper 45*. U.S. Department of Commerce: Washington, DC; 58.

Pederson N, Jacoby GC, D'Arrigo RD, Cook ER, Buckley BM. 2001. Hydrometeorological reconstructions for Northeastern Mongolia derived from tree rings: 1651–1995. *Journal of Climate* **14**: 872–881.

Richman MB. 1986. Rotation of principal components. *Journal of Climate* **6**: 293–335.

Rinn F. 1996. *TSAPWin: Time series analysis and presentation for dendrochronology and related applications*. Version 0.55 User reference, Heidelberg, 76.

Shao XM, Huang L, Liu HB, Liang EL, Feng XQ, Wang LL. 2005. Reconstruction of precipitation variation from tree rings in recent 1000 years in Delingha, Qinghai. *Science in China (Series D)* **48**(7): 939–949.

Sheppard PR, Tarasov PE, Graumlich LJ, Heussner K-U, Wagner M, Österle H, Thompson LG. 2004. Annual precipitation since 515 BC reconstructed from living and fossil juniper growth of northeastern Qinghai Province, China. *Climate Dynamics* **23**: 869–881.

Singh J, Park W-K, Radav RR. 2006. Tree-ring-based hydrological records for western Himalaya, India, since A.D. 1560. *Climate Dynamics* **26**: 295–303.

Stokes MA, Smiley TL. 1968. *An Introduction to Tree-Ring Dating*. The University of Chicago Press: Chicago, London; 73.

The Editing Committee of "The annals of Deqin County". 1997. *The Annals of Deqin County*. Yunnan Nationality Press: Kunming; 68, (In Chinese).

Webster PJ, Magana VO, Palmer TN, Shukla J, Tomas RA, Yanai M, Yasunari T. 1998. Monsoons: processes, predictability, and the prospects for prediction. *Journal of Geophysical Research* **103**(C7): 14,451–14,510.

Wigley T, Briffa KR, Jones PD. 1984. On the average value of correlated time series, with applications in dendroclimatology and hydrometeorology. *Journal of Climate and Applied Meteorology* **23**: 201–213.

Wu XD, Zhan XZ. 1991. Tree-ring width and climatic change in China. *Quaternary Science Reviews* **10**: 545–549.

Wu XD, Li ZY, Sun L. 1988. A preliminary study on the climatic change of the Hengduan Mountains area since 1600 A.D. *Advances in Atmospheric Sciences* **5**(4): 437–443.

Xu XD, Miao QJ, Wang J, Zhang XJ. 2003. The water vapor transport model at the regional boundary during the Meiyu Period. *Advances in Atmospheric Sciences* **20**: 333–342.

Yang MX, Yao TD, He YQ, Thompson LG. 2000. ENSO events recorded in the Guliya ice core. *Climatic Change* **47**: 401–409.

Zhang QB, Cheng GD, Yao TD, Kang XC, Huang JG. 2003. A 2,326-year tree-ring record of climate variability on the northeastern Qinghai–Tibetan Plateau. *Geophysical Research Letters* **30**(14): 1739, Doi: 10.1029/2003GL017425.